The phase diagram of the next-neighbour Ising model of the face-centred cubic lattice

Citation for published version:
Ackland, GJ 2023, 'The phase diagram of the next-neighbour Ising model of the face-centred cubic lattice', *European Physical Society Letters (EPL)*, vol. 142, no. 4, 41003, pp. 1-6. https://doi.org/10.1209/0295-5075/acd07c

Digital Object Identifier (DOI):
10.1209/0295-5075/acd07c

Published In:
European Physical Society Letters (EPL)

On the existence of an intermediate phase in the antiferromagnetic Ising model on the face-centered cubic lattice

Graeme J Ackland[†]

School of Physics and Astronomy, University of Edinburgh, Edinburgh EH9 3FD, United Kingdom

E-mail: `gjackland@ed.ac.uk`

Abstract. We use Monte Carlo simulation to determine the stable structures in the second-neighbour Ising model on the face-centred cubic lattice. Those structures are $L1_1$ for strongly antiferromagnetic second neighbour interactions and $L1_0$ for ferromagnetic and weakly antiferromagnetic second neighbours. We find a third stable "intermediate" antiferromagnetic phase with $I4_1$/amd symmetry, and calculate the paramagnetic transition temperature for each. The transition temperature depends strongly on second neighbour interactions which are not frustrated. We determine a sublattice structure suitable for solving this problem with mean field theory.

Keywords: Ising model, phase diagram, antiferromagnetic, Monte Carlo, face-centred cubic.

1. Introduction

The Ising model is perhaps the most famous model for magnetic interactions on a lattice. It is based on discrete spins located on discrete lattice sites interacting with nearby neighbours only. Despite its simplicity, it exhibits an order-disorder transition as a function of temperature. The face-centred cubic lattice (fcc, A1 in Strukturbericht designation), is one of the most commonly encountered structures in crystallography, and represents the most efficient packing of hard spheres. It has $Fm\bar{3}m$ symmetry with a single atom in the primitive cell. Thus the Ising model on the fcc lattice is one of the classic problems in condensed matter physics.

In the language of a magnetic system, the Hamiltonian, $\mathcal{H}$, for the Ising model with the nearest-neighbour (NN) interaction, J_1, and the next-nearest-neighbour (NNN) interaction, J_2, is

$$\mathcal{H} = -J_1 \sum_{\langle i,j \rangle'} S_i S_j - J_2 \sum_{\langle i,j \rangle''} S_i S_j - H \sum_{i=1} S_i, \quad (1)$$

where $\langle\rangle'$ stands for summation over NNs, and $\langle\rangle''$ for NNNs. Ising spins S_i are taken as ± 1. H is the magnetic field which we consider only in the ground state analysis; simulations are at zero field ($H = 0$). In the case of the fcc lattice, the sets of NN and NNN bonds have the same $Fm\bar{3}m$ as the lattice. The Hamiltonian in the above equation 1 can be analysed as a function of two dimensionless quantities: the ratio of the interactions relative to each other, and to the temperature.

$$\alpha = J_2/|J_1|, \qquad \beta^{-1} = T/|J_1|. \tag{2}$$

Without loss of generality, we choose units such that $|J_1| = 1$.

Calculation of phase stability in the antiferromagnetic Ising model is challenging because of the existence of many possible antiferromagnetic arrangements. Furthermore, the face-centred cubic lattice can be viewed as ABC stacking of triangular lattices, leading to frustration: when two spins on the triangle are different, the third cannot be simultaneously different from both. Furthermore, there exists an ordering without translational symmetry for the AFM triangular and fcc lattice which has lower energy than any periodic one (Fig.1), which inhibits nucleation and growth of periodic structures in a Monte Carlo simulation. Although the Hamiltonian $\mathcal{H}$ has full $Fm\bar{3}m$ symmetry, the antiferromagnetic arrangement of spins will normally have lower symmetry. The two main approaches to the problem are Monte Carlo simulation and mean field theories[1, 2, 3, 4, 5, 6, 7]. Monte Carlo correctly includes all correlation effects, within the 6912 independent sites, but being a numerical method cannot determine the phase boundary analytically[8, 9]. By contrast, effective mean field approaches[10] are typically built on cluster approaches which limits the spatial range of correlations. Crucial to this is the choice of sublattice structure, which restricts the possible antiferromagnetic symmetry-breakings. The sublattice structure must therefore be chosen with reference to possible solutions for $\mathcal{H}$.

Many previous authors have looked at the near-neighbour only case[11, 12, 13, 14, 15, 16, 17]. In our previous work[10], we analysed the case where α is positive, i.e. second neighbour interactions are ferromagnetic. We also considered non-zero field, creating a three-dimensional α, T, H phase diagram. In that system the possible phases are $L1_0$, $L1_2$ and paramagnetic. Those phases were examined in mean field theory using a conventional (4-atom) fcc cell in which the four sites are treated the independent sublattices. A superdegenerate point exists at H=4, T=0 where $L1_0$, and $L1_2$ are degenerate, as are a range of point and extended defects.

A recent paper by Jurčišinová and Jurčišin (JJ) entitled "Prediction of the existence of an intermediate phase in the antiferromagnetic J1-J2 system on the face-centered cubic lattice"[18] tackled the harder problem of $\alpha < 0$, where second neighbour interactions are also antiferromagnetic, simplifying matters by setting $H = 0$. Despite the title, they actually considered a Hamiltonian which has $Pm\bar{3}m$ symmetry with two inequivalent sites ($L1_2$ in Strukturbericht designation). To investigate symmetry-breaking due to antiferromagnetism, they used a three-site sublattice structure with one sublattice comprising the face-centres, and two sublattices on cube corners (Appendix

Structure	Free energy	Magnetization	Stability
$L1_0$	$-4J_1+6J_2$	0	AFM J_1, FM J_2
$I4_1$/amd	$-4J_1+2J_2$	0	J_1, AFM J_2,
$L1_1$	$-6J_2$	0	AFM J_2, $J_1 < -J_2$
Ferromagnetic	$12J_1+6J_2-H$	1	FM J_1, FM J_2
Paramagnetic	0	0	high T
Ferromagnetic[10]	$12J_1+6J_2-H$	1	high H
DO_{22} [10]	$2J_2-H/2$	1/2	AFM J_1, AFM J_2, medium H
AFM1[18] ($L1_2$)	$6J_2-H/2$	1/2	AFM J_1, FM J_2, medium H
AFM2[18] (m_C=1)	$12J_1+9J_2/2-3H/4$	3/4	nowhere
AFM2[18] (m_C=0)	-1.5J_2	0	nowhere

Table 1: Perfect crystal energies at T=0 from Eq. 1. Candidate phases from[10] AFM1 and AFM2 are from Ref [18]. "Stability" indicates the region of the phase diagram where the phase is expected. Horizontal line separates phases observed in this work from others reported elsewhere.

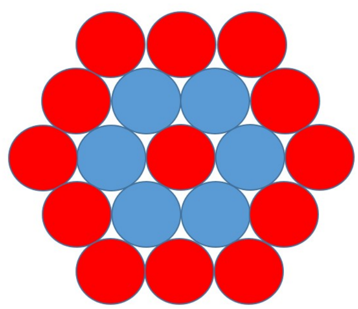

Figure 1: Aperiodic ordering on the triangular lattice with lower energy than any periodic order for nearest-neighbour AFM Ising model. Central site has six unlike neighbours: when extended in a bullseye pattern all other sites have four unlike neighbours. The lowest energy AFM periodic structures have four unlike neighbours at each site. The generalisation to fcc is straightforward - each subsequent layer is coloured to be different from the majority of sites below

Fig.5). They reported that the phase diagram has two "antiferromagnetic" phases (named AFM1 and AFM2) and a third "well-defined" intermediate phase. Here we investigate whether any intermediate state of the type found in the $Pm\overline{3}m$ Ising model is also present in the more familiar fcc lattice.

2. Ground State structures

First we consider only the T=0 case, attempting to identify the possible stable structures. According to the Third Law of thermodynamics, an ordered state must be

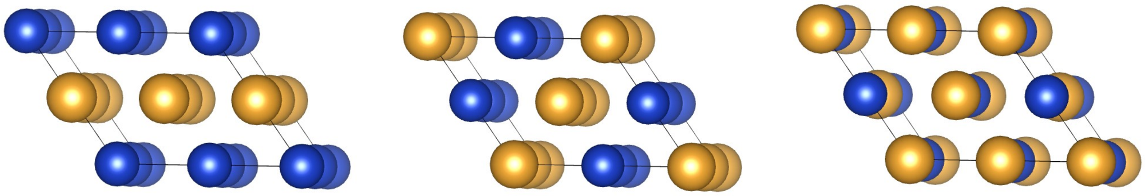

Figure 2: The FCC lattice in the $a = (110), b = (1\bar{1}0), c = (\frac{1}{2}, \frac{1}{2}, 1)$ setting viewed close to the b direction. Colouring shows the patterns of the various sublattice spin ordering corresponding to the $L1_0$, $L1_1$ and $I4_1$/amd structures.

the most stable. Identifying these candidate states is a necessary precursor to making a sensible definition of order parameters or sublattice structures. At T=0, these can be generated by hand, looking at colourings of sites on the appropriate lattice which maximise unlike first and/or second neighbours. Some orderings are long established from the near-neighbour problem and taken from previous work (here refs [18, 10] were used). Other structures were constructed by colouring-in drawings of the fcc lattice with a crayon, maximising the number of unlike second neighbours either absolutely ($L1_1$) or subject to maximised near-neighbours ($I4_1/amd$). The relevant phases are shown in Figure 2 with details given in Table 1 and the Appendix figures 2 and 5

If we consider the reported states of the JJ structures, we see that AF1 has $m_A = m_B = -m_C$. This is the $L1_2$ structure, which can be obtained in the four-sublattice model with $m_1 = m_2 = m_3 = -m_4$. In fcc, the $L1_2$ structure has a ground state energy which can be written in the three-sublattice decomposition as

$$\begin{aligned} E_{L1_2} &= E_A/8 + E_B/8 + 3E_C/4 \\ &= 0.125(12J_1 - 6J_2) + 0.125(12J_1 - 6J_2) + 0.75(-4J_1 - 6J_2) \\ &= -6J_2. \end{aligned}$$

or in the four-site decomposition as

$$\begin{aligned} E_{L1_2} &= E_1/4 + E_2/4 + E_3 + E_4/4 \\ &= 0.25(12J_1 - 6J_2) + 3 \times 0.25(-4J_1 - 6J_2) \\ &= -6J_2. \end{aligned}$$

For antiferromagnetic J_2 this is less stable than randomly oriented spins, and therefore $L1_2$ (AF1) should not appear in this region of the phase diagram, since it is not stable at T=0, and has lower entropy than the disordered paramagnetic state. DO_{22} is always more stable than $L1_2$, but even it may only be stabilised by an external field[10].

We can contrast this with the $L1_0$ phase which comprises alternating (001) planes of different spins; using our sublattice structure it is $m_1 = m_2 = -m_3 = -m_4$, but $L1_0$ cannot be represented within the three-sublattice assumption. In $L1_0$ all sites have equal energy $E = -4J_1 + 6J_2$. This is the unique stable state at zero field for ferromagnetic

J_2, and extends some way into the antiferromagnetic J_2 region (Figure 3. Clearly, for $6J_2 > 4J_1$ this L1_0 structure has higher than zero, so some other ordered phase must exist which favours unlike second neighbours.

A candidate for this phase is L1_1: a layered structure with alternating (111) close-packed planes of opposite spins, symmetry $R\overline{3}m$. It cannot be defined based on either of the sublattices considered above. Relative to the conventional fcc cell, it is a two atom cell with a=(1/2,-1/2,0), b=(-1/2,0,1/2), c=(0,1,-1), with basis atoms at (0,0,0) and (0,0,1/2) which define the sublattice. This structure has T=0 energy -6J_2, and so becomes degenerate with L1_0 at $J_2 = J_1/3$.

It seemed unlikely that L1_0, which has all NNN aligned, could persist when J_2 is antiferromagnetic. For near-neighbour only interactions L1_0 has zero-energy stacking faults[10], and by considering an array of stacking faults we found an intermediate phase with I4_1/amd symmetry which does not appear in the Strukturbericht designation. This is degenerate with L1_1 at $J_2 = J_1/2$ and L1_0 $J_2 = 0$, and more stable between those values.

We note that in the limit $J_1 \to 0$ the fcc structure breaks into four unconnected simple cubic lattices, which can be made independently antiferromagnetic in the B1 (NaCl) structure without frustration. L1_1 can be viewed as four interpenetrating NaCl lattices.

3. Numerical simulations

We ran Metropolis Monte Carlo[19] simulations on a 12x12x12x4 atom supercell. The model parameters are J_2 and T and there are two cases: ferromagnetic $J_1 = 1$ and antiferromagnetic $J_1 = -1$. No external field was applied ($H = 0$). Updates were single-site flips, of randomly-chosen sites. At each temperature we equilibrate for 10^6 attempted flips and collect data for 10^9.

In Figure 3 we show the phase diagram found by monitoring the temperature variation of fluctuations in the energy:

$$c(T) = \langle \mathcal{H}^2 \rangle - \langle \mathcal{H} \rangle^2 \tag{3}$$

and detecting peaks therein. To detect transitions between ordered phases we monitor fluctuations in the NNN contribution to the energy only.

The simulations revealed just four distinct ordered phases, all of which were as anticipated from the analytic ground state calculations.

- ferromagnetic for $J_1 > 0; J_2 > -J_1$,
- L1_0 for $J_1 < 0; J_2 > 0$,
- I4_1/amd for $J_1 < 0; -J_1/2 < J_2 < 0$,
- L1_1 for $J_1 < 0; J_2 < -J_1/2$, and for $J_1 > 0; J_2 < -J_1$.

The AFM1 and AFM2 structures found by JJ on their $Pm\overline{3}m$ lattice are not observed in fcc, $Fm\overline{3}m$ with antiferromagnetic second neighbours. Our intermediate I4_1/amd structure is also different from the JJ intermediate structure.

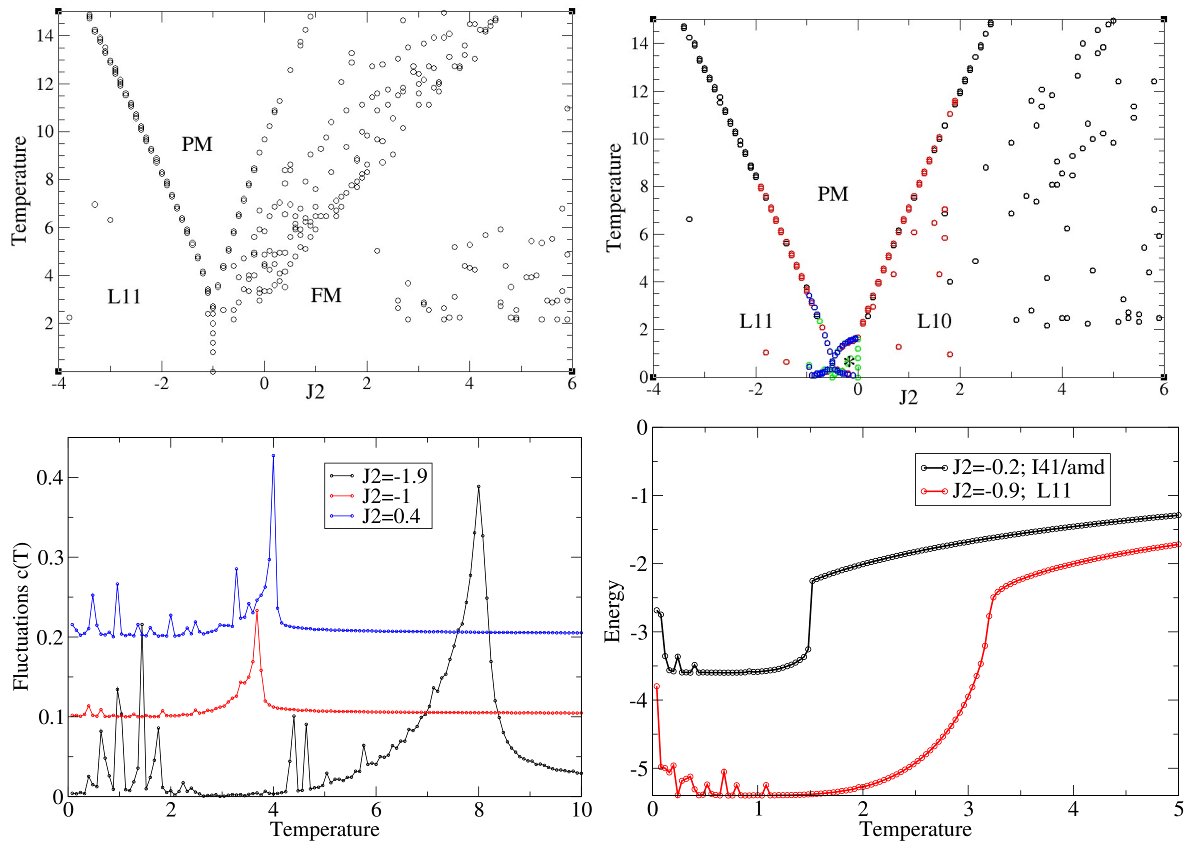

Figure 3: Phase diagram for (top left) Ferromagnetic $J_1 = 1$ (top right) Antiferromagnetic $J_1 = -1$. Points indicate the (J_2, T) tuple for the two highest values of peaks in c: for the PM transition line this is a lambda peak, within ordered phase is comes from annealing a domain structure. Colours indicate starting configuration: black: PM, red: FM, blue $L1_0$, green $L1_1$. Star indicates the small region of $I4_1$/amd. (bottom) typical plots of $c(T)$ and $\mathcal{H}(T)$ for $J_1 = -1$, and energy for showing sharp "annealing" peaks at lower in the ordered phases, which in these cases are not large enough to appear in the phase diagram and lambda peak at the paramagnetic transition.

Peak detection is not completely straightforward, because a high variation of $\mathcal{H}$ can occur if there is a domain structure which rearranges itself during a simulation. Such an event produces a bimodal distribution and consequent high value for $(\langle \mathcal{H}^{\in} \rangle - \langle \mathcal{H} \rangle^2)$ at a single temperature, whereas a thermodynamic phase transition produces a characteristic lambda transition across a range of temperatures. For this reason, $c(T)$ cannot always be associated with a specific heat capacity. To address this, we plot in Fig.3 the temperatures corresponding to the two highest values of $c(T)$ as points on a graph of J_2 vs T. This traces out the phase boundaries with a sharp line, and also shows a diffuse region corresponding to the "annealing temperature", at which point the single-flip algorithm is able to anneal out a domain structure. We also plot examples of $c(T)$ and $\mathcal{H}(T)$ from single runs which show the domain formation events as single peaks.

In all the AFM phases, the sites are equivalent except for the sign of the spin, so the sublattice magnetisation is simply the square root of fraction of the T=0 binding energy (i.e. energy with negative sign).

The phase lines are rather straight, with the PM transition temperature lowest at the "maximally frustrated" value of J_2 where two ordered structures are degenerate.

4. Sublattice structures

A mean field treatment of the antiferromagnetic second neighbour Ising model will require a sublattice decomposition which permits all possible ground states: alternating (001) layers and alternating (111) layers, and the $I4_1/amd$. Each have two independent sublattices, so a supercell which can describe them all requires at least eight sublattices. One such structure is shown in Fig.2. Compared to the conventional fcc cell it has a=(1,1,0) b=(1,-1,0) c=($\frac{1}{2}$, $\frac{1}{2}$,1). To include $L1_2$ and DO_{22} structures a still larger set of sublattices is needed, based on a 16 atom cell a=(1,1,0) b=(1,-1,0) c=(0,0,2). (Table 2)

The changing domain structure of the Monte Carlo simulation precludes assignment of sites to sublattices, but one can obtain a mean-field estimate of sublattice magnetisation m from inverting Eq.1 using the T=0 energies in Table 1, i.e. $m = \sqrt{\mathcal{H}(T)/\mathcal{H}(0)}$. This is valid only in the ordered phase, and follows typical Ising-model behaviour.

5. Discussion and conclusions

We find four different ordered phases in the second-neighbour (J_1, J_2) Ising model on the fcc lattice: Ferromagnetic fcc, and ordered AFM phases $I4_1$/amd, $L1_1$, and $L1_0$. All of these are stable at zero temperature, and with increased temperature, all transform directly to a paramagnetic state.

Numerical simulations show that the stable structures with antiferromagnetic J_1 interactions all have zero magnetisation (assuming H=0). Spontaneous magnetisation is observed only for ferromagnetic J_1.

The Monte Carlo simulations also reveal a reasonably well-defined temperature at which specific defects, such as stacking faults and microdomains, start to be generated or annealed out. While interesting, it is likely that this temperature is sensitive to the single-flip algorithm, and its exact position is both ill-defined and sensitive to finite size effects[9].

A recent mean field calculation, which also reported two AFM states and an intermediate structure in the "face-centred cubic lattice" was, in fact, considering a different lattice, i.e. $L1_2$ with no interactions between face-centred sites. There is no discrepancy between these results, but we note that the 3-sublattice decomposition assumed in that work does not permit the $L1_0$, $I4_1$/amd and $L1_1$ groundstates of the antiferromagnetic fcc lattice, and cannot sensibly be applied to the Hamiltonian considered here. Similarly, the 4-sublattice decomposition which was used previously[9]

x	y	z	$L1_0$	$L1_1$	$I4_1$/amd	$L1_2$	DO_{22}	FM
0	0	0	1	1	1	1	1	1
1/2	0	0	1	1	-1	1	1	1
1/2	1/2	0	1	-1	1	1	1	1
0	1/2	0	1	-1	-1	1	1	1
1/4	1/4	1/4	-1	-1	-1	-1	-1	1
1/4	3/4	1/4	-1	1	1	1	1	1
3/4	1/4	1/4	-1	-1	1	1	1	1
3/4	3/4	1/4	-1	1	-1	-1	-1	1
0	0	1/2	1	-1	-1	1	1	1
1/2	0	1/2	1	-1	1	1	1	1
1/2	1/2	1/2	1	1	-1	1	1	1
0	1/2	1/2	1	1	1	1	1	1
1/4	1/4	3/4	-1	1	1	-1	1	1
1/4	3/4	3/4	-1	-1	-1	1	-1	1
3/4	1/4	3/4	-1	1	-1	1	-1	1
3/4	3/4	3/4	-1	-1	1	-1	1	1

Table 2: Fractional positions in tetragonal supercell with $a = b = \sqrt{2}$, $c = 2$ relative to conventional fcc cell, and associated ground state spins for structures in the phase diagram.

in the ferromagnetic J_2 case would also be inappropriate for the antiferromagnetic J_2 case. We demonstrate that an effective mean-field theory treatment covering all possibilities for the second-neighbour fcc Ising model would require eight sublattices.

The paramagnetic transition temperature is strongly dependent on J_2, even if J_1 is held fixed. It takes its lowest value at the point where two competing ordered structures have identical ground-state enthalpy. This is true regardless of whether T is measured in units of $|J_1|$ or an average interaction weighted by number of neighbours, i.e. $|J_1|+|J_2|/2$. The disproportionate effect of J_2 on the transition temperature follows from the absence of frustration in NNN interactions.

Acknowledgement

Funding for this work was provided by ERC grant Hecate. The author thanks Hossein Ehteshami for bringing this problem to his attention.

6. References

[1] Binder K 1980 Physical Review Letters **45** 811

[2] Beath A and Ryan D 2005 Physical Review B **72** 014455
[3] Beath A and Ryan D 2006 Physical Review B **73** 214445
[4] Beath A and Ryan D 2007 Journal of applied physics **101** 09G102
[5] Polgreen T L 1984 Physical Review B **29** 1468
[6] de Sousa J R and Plascak J 2008 Physical Review B **77** 024419
[7] Phu X P, Ngo V T and Diep H 2009 Physical Review E **79** 061106
[8] Ackland G J 2006 Physical Review Letters **97** 015502
[9] Ehteshami H and Ackland G J 2021 Journal of Physics: Condensed Matter **33** 345402
[10] Ehteshami H and Ackland G J 2020 Journal of Physics: Condensed Matter **32** 385402
[11] Mackenzie N and Young A 1981 Journal of Physics C: Solid State Physics **14** 3927
[12] Finel A and Ducastelle F 1986 EPL (Europhysics Letters) **1** 135
[13] Gahn U 1986 Journal of Physics and Chemistry of Solids **47** 1153–1169
[14] Mazel A 1988 Theor. Math. Phys.;(United States) **74**
[15] Zarkevich N A, Tan T L, Wang L L and Johnson D D 2008 Physical Review B **77** 144208
[16] Lundow P H, Markström K and Rosengren A 2009 Philosophical Magazine **89** 2009–2042
[17] Stübel R and Janke W 2018 Physical Review B **98** 174413
[18] Jurčišinová E and Jurčišin M 2022 Europhysics Letters **139** 26001
[19] Metropolis N, Rosenbluth A W, Rosenbluth M N, Teller A H and Teller E 1953 The journal of chemical physics **21** 1087–1092

7. Appendix- previous sublattice decompositions

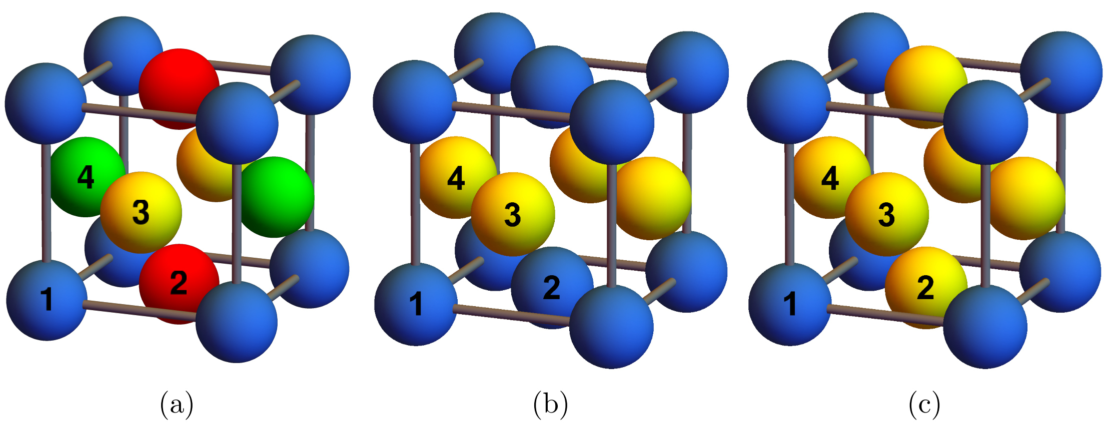

Figure 4: (a) Four-sublattice decomposition based on conventional unit-cell of FCC. FCC lattice can be considered as four interpenetrating simple cubic (SC) lattices which each SC lattice here is denoted by a different colour. (b) $L1_0$ is represented by $A = m_1$ (●) $= m_2$ (●), $B = m_3$ (●) $= m_4$ (●), and (c) $L1_2$ by $A = m_1$ (●), $B = m_3$ (●) $= m_2$ (●) $= m_4$ (●).

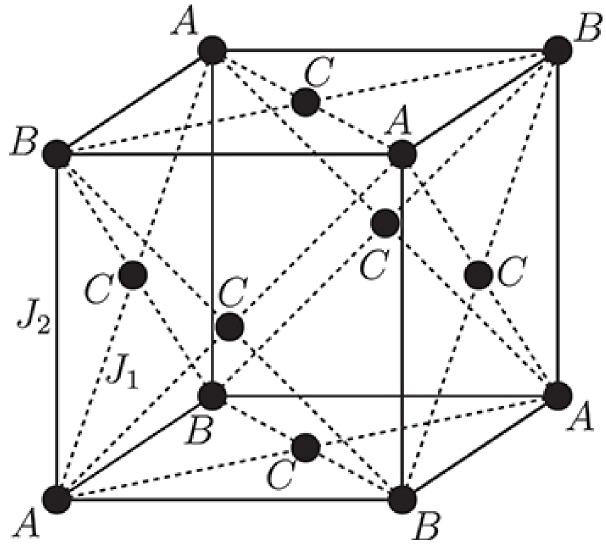

Figure 5: Three-sublattice decomposition based on conventional unit-cell of FCC. Figure taken from Jurčišinová and Jurčišin [18]. In discussion with those authors afte rthe current paper was complete, it transpires that the lattice they consider has *only* the interactions shown in the figure, i.e. no interactions between atoms on the face-centre C sublattice. Moreover, the corner sites were doubly-weighted